

## Strength Enhancement of cellular structures through selective reinforcement of elements based on analytical modeling

Naresh Koju\* † and Li Yang\*

\*Department of Industrial Engineering, University of Louisville, Louisville, KY 40292

†Email: [naresh.koju@louisville.edu](mailto:naresh.koju@louisville.edu)

### Abstract

This work investigates the strength enhancement of 2D cellular structures via individual element thickness optimization based on the analytical model for critical elements. To focus on the investigation of the enhancement method, a rather simplified perfectly elastic material property was assumed, and an analytical model was utilized to identify the critical element of several cellular structure designs. Stepwise element thickness enhancement was utilized to investigate the effectiveness of overall strength enhancement. The results indicate that the strength of cellular structures can be improved by selectively reinforcing critical elements. In addition, the enhanced cellular structures also exhibit altered fracture failure characteristics that could potentially be exploited for more application objectives.

**Keywords:** Lattice structure, strength enhancement, analytical model, failure propagation/pattern

### 1. Introduction

The concept of periodic cellular structures for lightweight design has been utilized for different applications. Generally, there exists a trade-off between different mechanical properties such as strength, energy absorption capacity, and deformation stability (smoothness of stress-strain curve), which can potentially impose restrictions on multi-objective designs [1]. In most cases, the uniform patterning-based design could not satisfy the requirements due to the heterogeneous response within the structures, and therefore additional design optimization with local structural elements such as thin struts and thin walls are often needed. Most of the current design approaches for the mechanical strength enhancement of cellular structures either take an explorative approach or utilize optimization algorithms. The explorative approach often draws inspiration from natural designs and generally involves random design trials to identify the optimum designs. Some specific examples include novel unit cell design [2, 3], graded structural design [4], nature-inspired design such as bio-inspired [5], and crystal-twinning inspired designs [6]. The design exploration space can include various aspects/variables such as overall architecture, constituent material, microstructure, or a combination of them [7-11]. The explorative approach can often provide useful insights into the design concepts and structural enhancement mechanisms. On the other hand, it could also be less efficient for the purpose of optimization due to the rather long “search” process. In comparison, optimization algorithm-based design approaches such as topology optimization tend to be more effective in improving the mechanical strength of a given structure [12-14]. However, the optimization algorithms generally provide very limited design insights owing to their iterative numerical optimization process.

This study aims not only to attempt to achieve design optimization but also to allow for the investigation of design insights for the strength enhancement of several representative cellular structure designs. Specifically, analytical models for 2D cellular structures were established and subsequently employed to reinforce the thickness of critical elements in a stepwise manner, until the intended strength requirements were achieved. The analytical model also provides a predicted failure propagation pattern. Two design optimization strategies were investigated, one focusing on the most critical elements, and the other one focusing on the entire failure pathway. The effectiveness and efficiency of the two strategies were compared to provide additional insights into the property enhancement mechanism.

## 2. Modeling of cellular lattice structures

### 2.1. Displacement method for strength enhancement of lattice structures

Wu and Yang [15, 16] developed analytical models based on the direct stiffness method for the modeling and analysis of 2D and 3D lattice structures, which was utilized as the foundation for this work. In this study, the analytical models were further parameterized to allow for more efficient design with allowance for the design variation of both global parameters such as the unit cell topology, the number of unit cells along different directions, and material properties, as well as individual element thickness. To allow for the efficient establishment of the stiffness matrix for large-size cellular designs, initially, the element connectivity network is created with redundant nodes based on the unit cell pattern (Fig. 1a), then the redundant nodes are eliminated by utilizing the nodal coordinates (Fig. 1b).

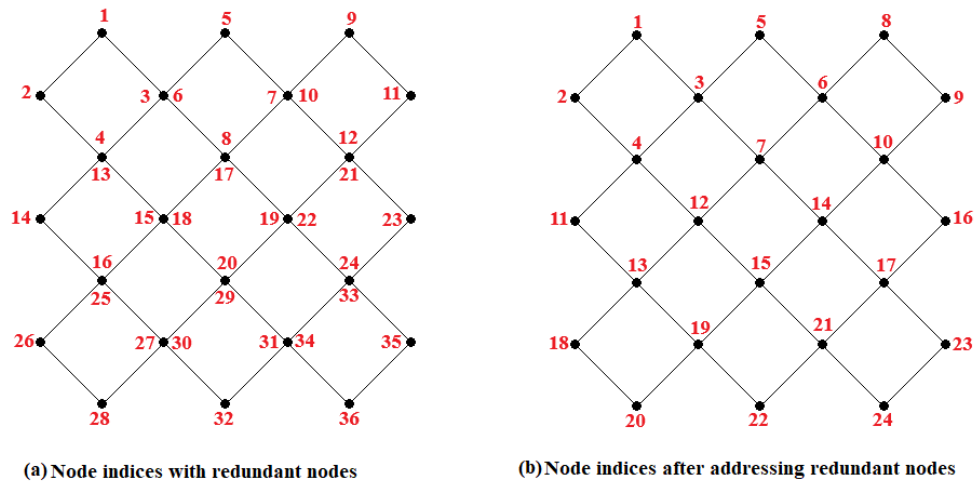


**Fig. 1** Nodal indexing approach for element connectivity

Similar to previous studies, all elements in the lattice structures were modeled by Timoshenko Beam theories and stiffness matrix assembly was employed to construct the global stiffness matrix. The isotropic brittle material model was employed for this study to avoid the potential complication of material effects. Three 2D cellular designs, including diamond, triangular, and auxetic unit cells, were used for investigation. The selection of these unit cells was based on two design mechanisms: (1) positive/negative Poisson's ratio and (2) stretching-/bending-dominated structure. Material properties of perfectly elastic isotropic Ti6Al4V (elastic modulus 114GPa, ultimate strength 1050MPa, and shear modulus 44GPa) were used for the analytical model and

subsequent finite element simulation studies. For the study, the baseline unit cell geometry (regardless of unit cell design) included elements with a length ( $L$ ) of 8mm, thickness ( $t$ ) of 1mm, width of 10mm, and height ( $H$ ) twice the length. In addition, the angle between the two elements ( $\theta$ ) is  $45^\circ$ ,  $60^\circ$  and  $90^\circ$  for auxetic, triangular, and diamond structures respectively, as illustrated in Fig. 2.

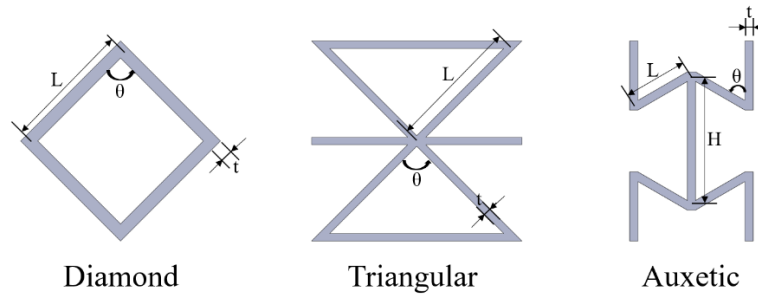


**Fig. 2** Different 2D unit cells indicating geometry design parameters

The original strength of each structure was utilized as a baseline for the strength reinforcement, and the objective was set as percentage strength reinforcement values in the model. The detailed steps in the analytical model program are presented in the flowchart (Fig. 3). The reinforcement steps involve the construction of full-size cellular structure analytical model based on stiffness matrix method, identification of critical elements, step-wise reinforcement, re-analyzing the structure to quantify the reinforcement effect, repeat the reinforcement step if strength requirement has not been met, and finally the plotting of fracture failure pattern. In this study, the critical element refers to the element with the highest elemental stress in the structure during each iteration, and these elements are reinforced by thickening their cross-sectional area (i.e., increasing thickness).

Two reinforcement strategies were evaluated with the 5x5 pattern for the three unit cell cells. Based on the results, the more efficient strategy was selected for the rest of the study. In each iteration, the first strategy only reinforces the first set of critical element(s), whereas the second strategy reinforces all the critical elements that would failure for a complete failure (structure disintegration) simultaneously. Each iteration included step-by-step element reinforcement by a certain thickness value, which terminates when the reinforcement objective was met. Since a cellular structure can have multiple critical elements simultaneously (e.g., due to symmetry), all these critical elements were reinforced in the same step. An example of the reinforced structure architecture using the first strategy is presented for a 3x3 diamond structure in Fig. 4, which clearly shows the reinforcement of the set of the most critical element(s).

The efficiency of reinforcement was evaluated in terms of weight increment in reference to original structure and number of reinforced elements involved. For consistency, the Ti6Al4V material density of 4.43g/cc was utilized for the weight increment calculations. Achieving the same strength reinforcement effect with minimal weight increment and reduced number of reinforced elements was considered more favorable in this study.

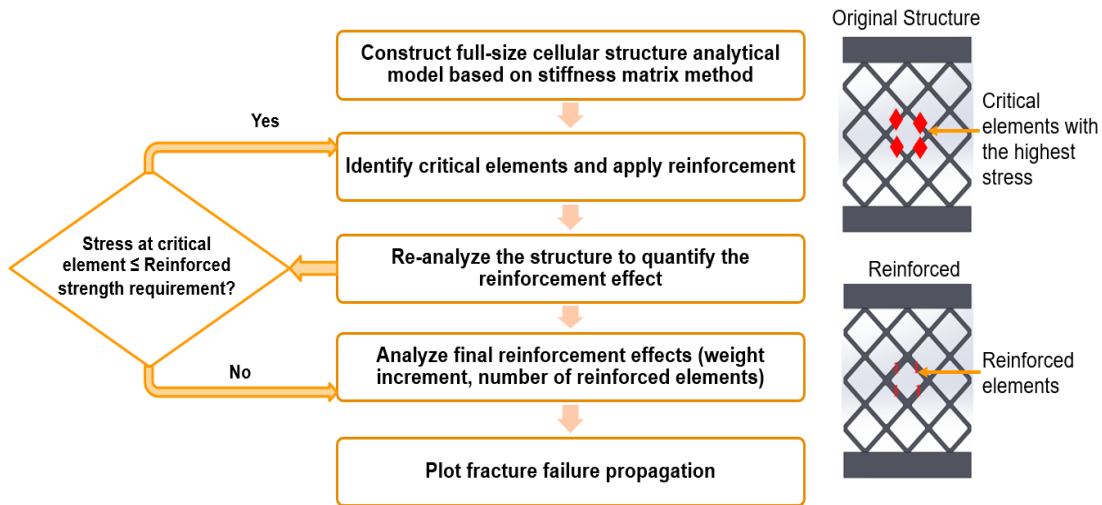


**Fig. 3** Analytical Modeling program flowchart

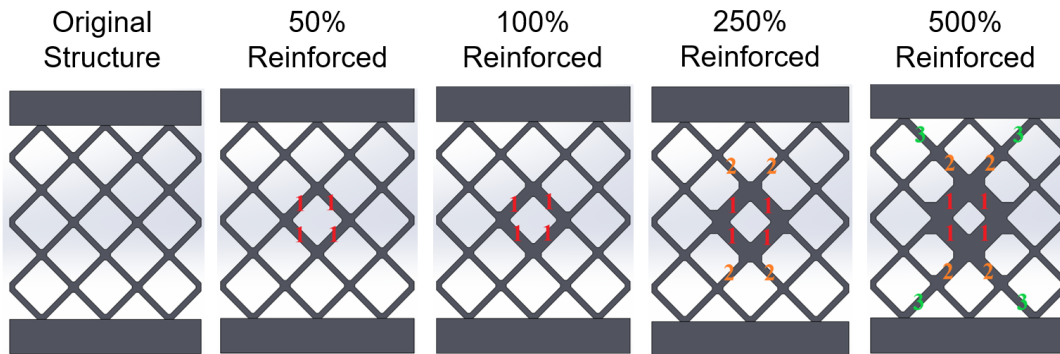


**Fig. 4** Architecture of 2D diamond structure at different reinforcement levels

## 2.2. Modeling of progressive failure of lattice structures

To investigate the failure progression, the most critical element, which was identified as the element with the highest stress level, will be removed from the model during each failure step analysis. If there are multiple critical elements, the element with the lowest index was selected. This iterative process gradually removes structural elements until the entire structure fails completely, indicated by zero nominal structural stress. Instantaneous failure of multiple elements, which was considered to be low probability in reality due to the presence of other noise factor (e.g. quality variability), was also characterized from the elemental stress values.

## 2.3. Model Verification

To further verify the analytical modeling approach, finite element analysis (FEA) was employed with the 3x3 diamond pattern. Three levels of reinforcement including 50%, 100%, 250%, and 500% were utilized for verification. The model was initially validated with ANSYS static analysis. The model was set up with one end fixed and pressure of 8.115MPa (corresponds to the first failure nominal stress value from the analytical model) applied to the other end (Fig.5a). Each reinforced structure was modeled based on the reinforced element(s) information obtained from the analytical model using the first reinforcement strategy (most critical struts only). The mesh sensitivity study

with maximum von-mises stress performed on the original structure showed mesh convergence between 0.2mm and 0.3mm mesh size (Fig. 5b). Thus, further FE analyses for reinforced structures were carried out with a mesh size of 0.25mm. The simulation results are presented in Fig. 6. With the increase in reinforcement level, the local stress concentration gradually decreased, implying increasing higher strength of the overall cellular structure and thus the effectiveness of the reinforcement strategy. It is also noted that the overall structural reinforcement effect was significantly higher than stress concentration reduction with individual elements, indicating the presence of non-local enhancement effects.

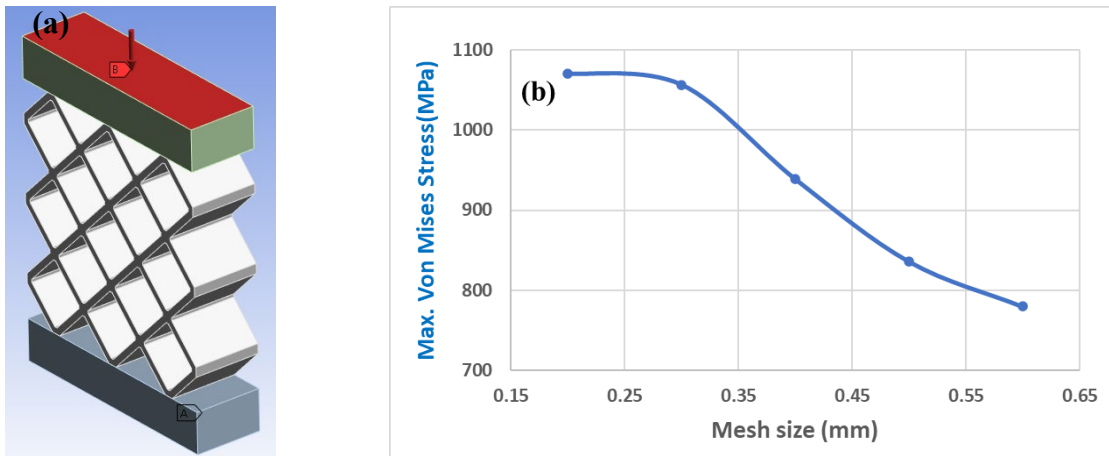


Fig. 5 (a) boundary Conditions, (b) mesh sensitivity analysis

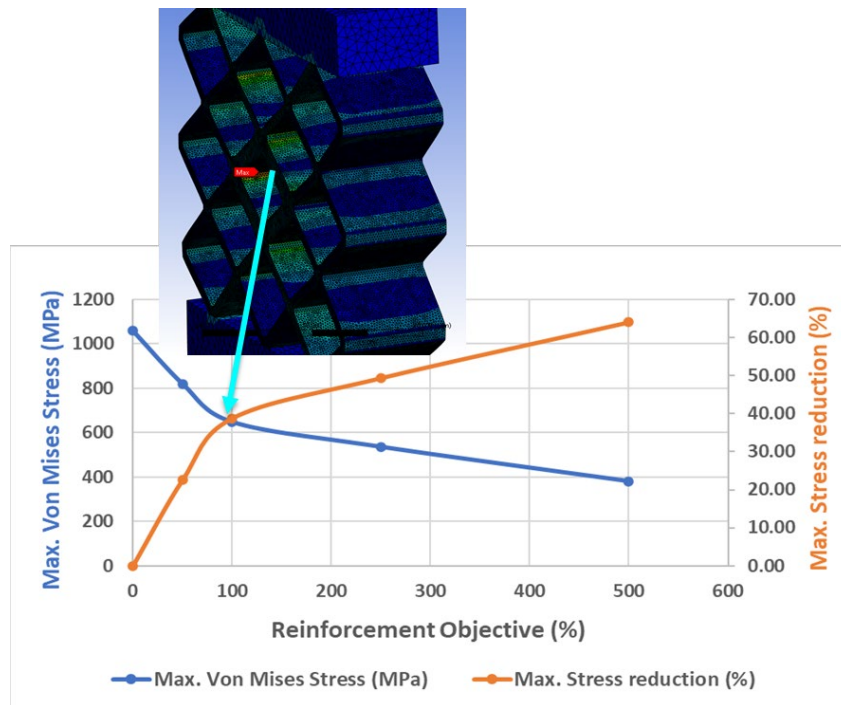
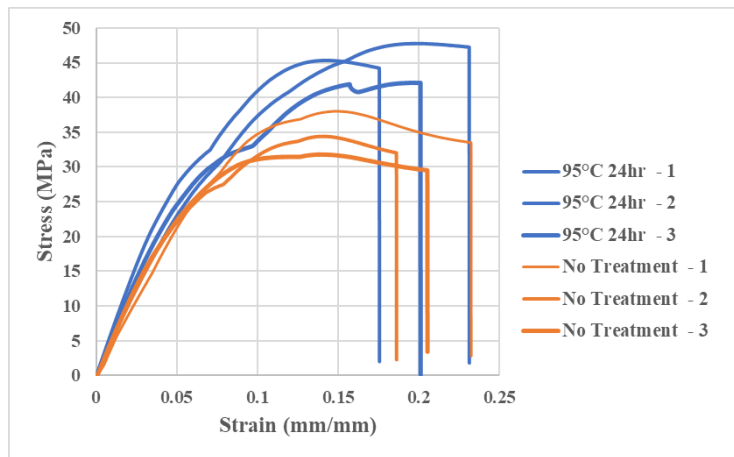


Fig. 6 Local maximum stresses with different reinforcement objectives

For the experimental model verification, the cellular lattice structures were fabricated by a Formlab Form-2 vat photopolymerization printer using Clear EPAX Hard Resin photopolymer. The

material exhibits plasticity, which differs from the brittle material model used by the analytical model in this study. Therefore, to reduce plasticity, the samples were exposed to a temperature of 95°C for 24hrs and quenched immediately to room temperature for embrittlement. The effect of the heat treatment process can be observed from the tensile testing with the tensile coupons in Fig. 7. The experimental compressive strength test samples and test results are presented in Fig. 8-9. Diagonal failure and inverted V-shaped failure were observed in the original and 50% reinforced designs, while the failure patterns for the 100% and 500% reinforced designs could not be discerned due to the catastrophic disintegration of samples upon fracture. The increase in strength with increased reinforcement level can be observed, however, the actual strength reinforcement was observed to be significantly lower compared to the analytical model expectations. For the 500% reinforcement design, only ~190% strength enhancement was obtained experimentally. Part of this result can be explained by the use of the 0.3mm chamfer with the designs due to the consideration of manufacturability. The chamfer feature effectively provides reinforcement effects to the structure, and it is also more significant for the original structures. However, the effect of chamfer only contributes to the discrepancy to a limited extent. The other possible contributing factor is the plasticity with the material even after the embrittling heat treatment. The plasticity could potentially result in less stress concentration in the critical elements and thus less reinforcement effectiveness. It was also interesting to note that the elongation at break decreased initially but increased later with the increase of reinforcement level.



**Fig. 7** Tensile test results of heat-treated and non-heat-treated samples (3 replicates each)

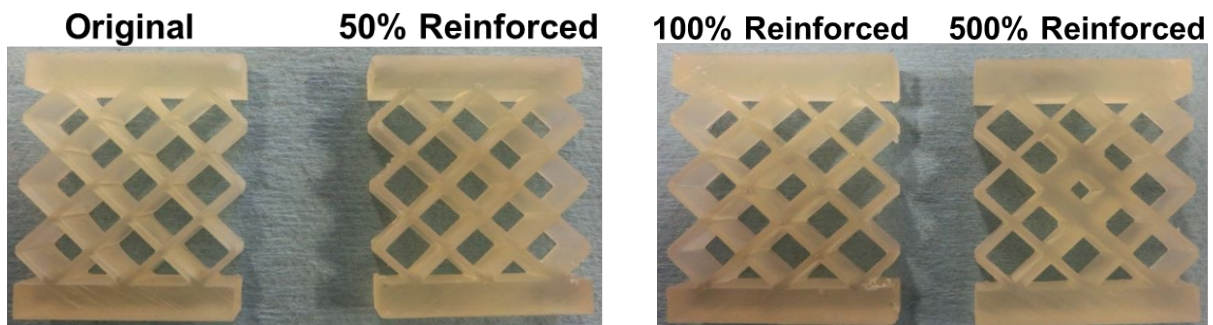


**Fig. 8** Compression test samples

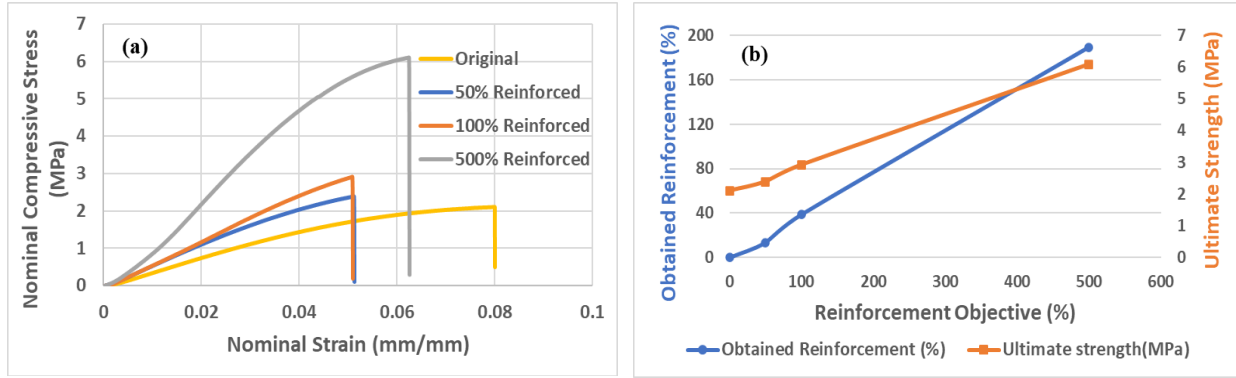


**Fig. 9** (a) Compression test stress-strain curves of different structures, (b) comparison between experimental and analytical results

### 3. Results and Discussion

#### 3.1. Effectiveness of reinforcement strategies

A comparison between two reinforcement strategies was performed at 100% reinforcement level based on analytical models. The stress-strain curves and effectiveness represented in terms of weight increment (%) and number of reinforced elements are shown in Fig. 10. The stress-strain curves indicate the equivalency of both methods in terms of the maximum structural nominal strength. However, there exist significant differences in both the number of elements to be reinforced and the overall weight increment between the two reinforcement strategies at every reinforcement level. Although the structure fracture propagation involves multiple levels of element fractures, from the stress-strain curve of the original structure it can be seen that the first fracture step is most significant. This explains why the reinforcement of all the elements across the entire fracture propagation is not most efficient. Based on these results, the first reinforcement strategy that reinforce only the most critical elements in each iteration was identified to be a more efficient approach and was selected for all further investigations.

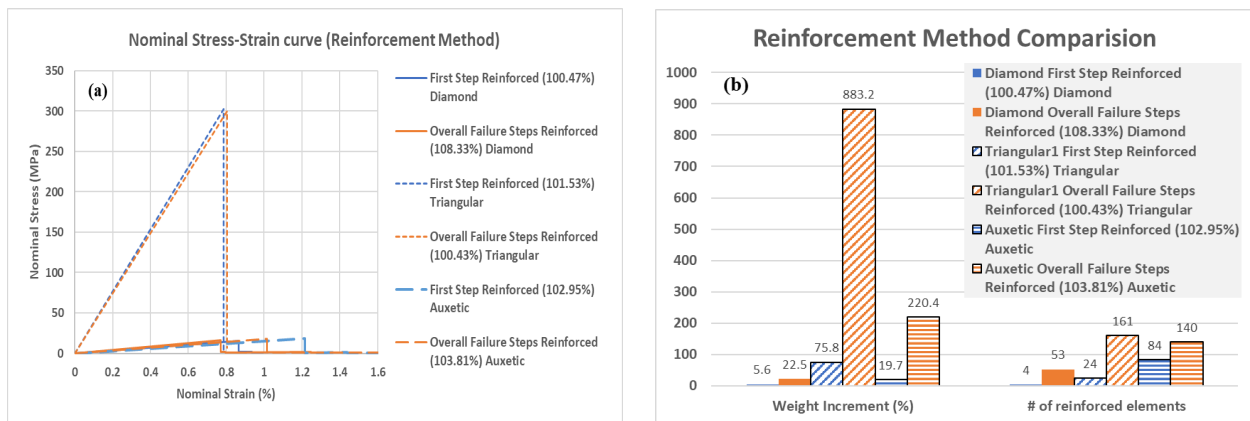


**Fig. 10** (a) Nominal stress-strain curves, (b) effectiveness comparison of reinforcement methods

### 3.2. Unit cell effect

As expected, stress-strain curve for 100% reinforced structures showed similar trend as their original counterpart. Additionally, auxetic and triangular structures showed the highest number of reinforced elements and weight increment respectively (Fig. 11).

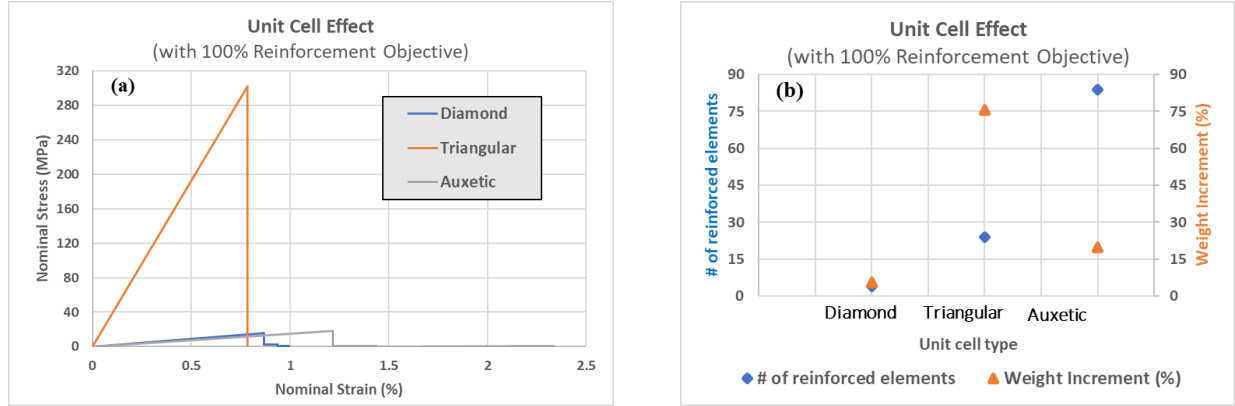


**Fig. 11** Unit cell topology effect at 100% reinforcement objective

The reinforced structures of all three-unit cell types showed the changes in the fracture pattern when compared to the original structure failure, indicating the significant influence of reinforcement in failure propagation (Fig. 12). For diamond structure, the fracture pattern transitioned from V-shape to inverted V-shape. For triangular structure, the fracture propagated more towards the thickness direction of the part. For auxetic structure, the propagation pattern changes from middle plane region to the boundary regions.

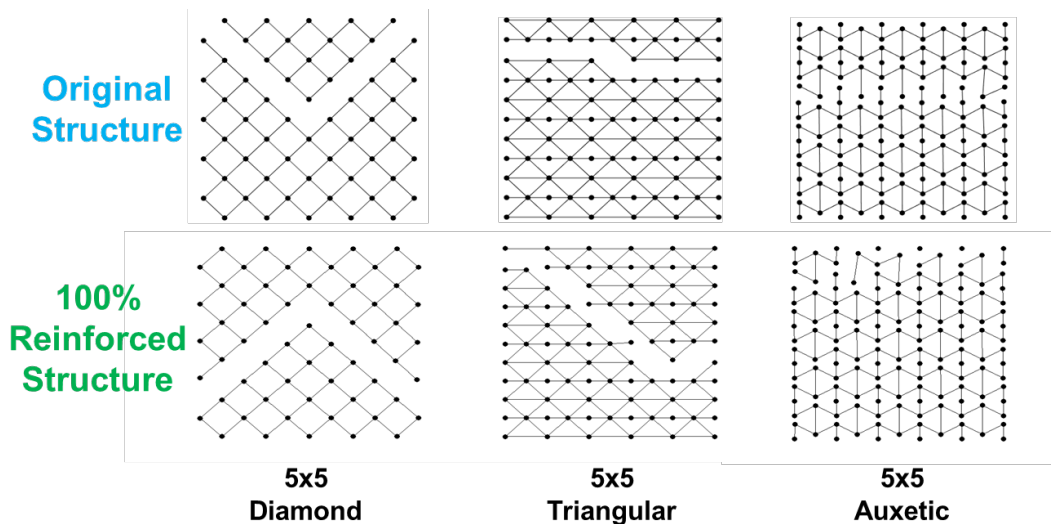


**Fig. 12** Failure pattern of different unit cells for original and 100% reinforced structure

### 3.3. Reinforcement performance

The effectiveness of the reinforcement method was evaluated at different levels ranging from 5 to 500% with the analytical model. Fig. 13 shows the stress-strain curves for reinforced structures. Similar to the experimental results obtained in the model verification, the elongation

at break values for all the design types decreased initially with increase in reinforcement level and later increased at higher reinforcement levels. The failure patterns are shown in Fig. 14. For diamond structure, there exists a clear transition from a diagonal failure pattern to V-shaped pattern for diamond structure, which agrees with the experiment. This transition is expected due to the increasingly spread locations of the critical/reinforcement elements from the center unit cell with the increase in reinforcement level (as shown in Fig. 4) and/or the stochasticity of the failure location due to structural symmetry. On the other hand, no strict transitions can be observed on triangular and auxetic structures at different reinforcement levels.

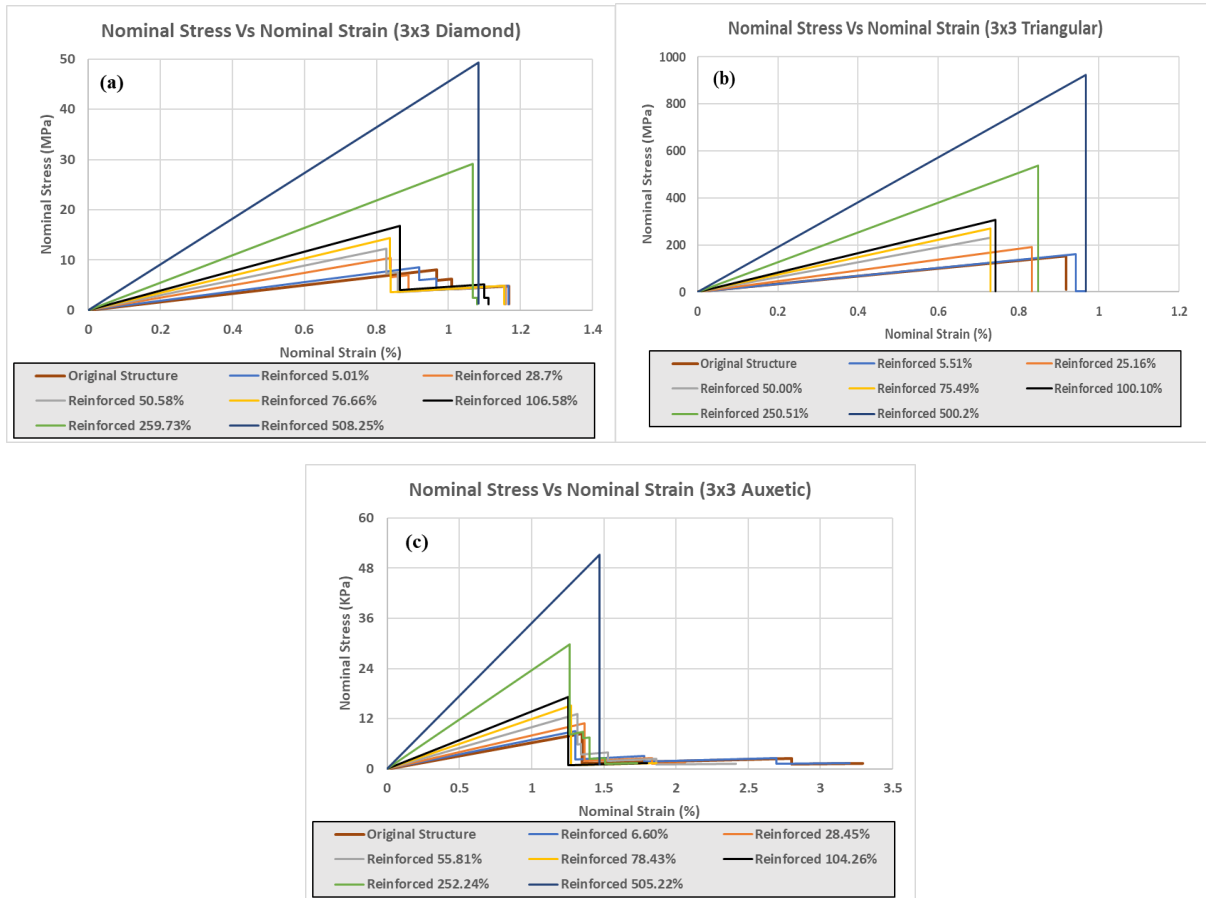


**Fig. 13** Stress strain curves at different reinforcement levels in different structures

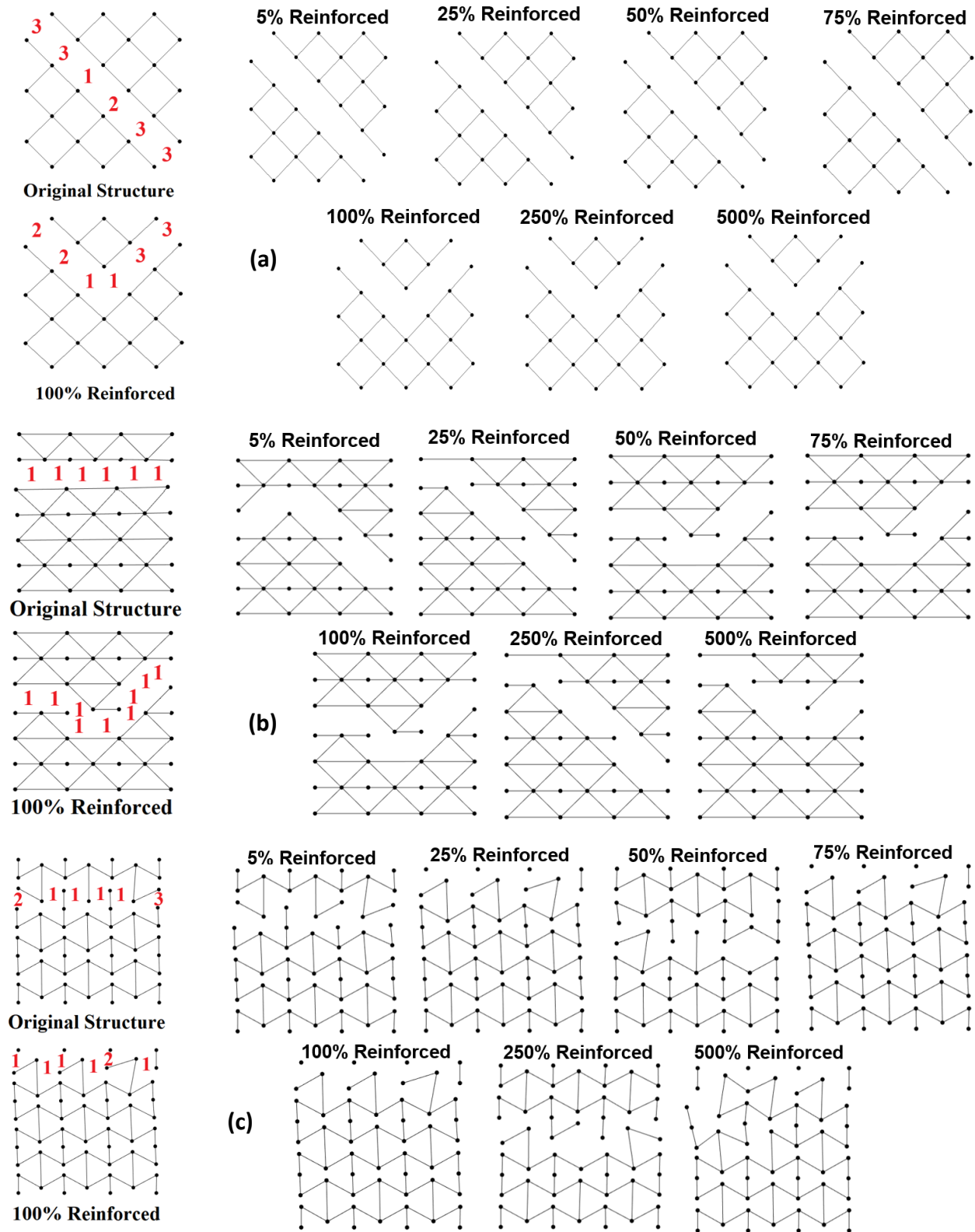


**Fig. 14** Failure patterns at different reinforcement levels (a) diamond structure, (b) triangular structure, (c) auxetic structure

Fig. 15 shows the weight increment and number of reinforced elements for different cellular designs at different reinforcement levels. All the unit cell topology studied in this work exhibited approximately linear weight increment trend with increase of the strength enhancement level, owing to either the continued increment in the number of reinforced elements and/or continued thickening of same critical elements. The diamond structure had same critical elements continuously reinforced till 100% reinforcement level, and at higher reinforcement levels additional elements become involved. On contrast, both triangular and auxetic structure have increased number of elements getting reinforced at increased level of reinforcement objective until it reaches a certain threshold. Afterwards the same set of elements continue to be further reinforced. The concentrated reinforcement locations over a large range of reinforcement levels could be of significance from a design perspective. On one hand, the high level of criticality of these elements makes it easier for the design reinforcement effort. On the other hand, however, this also indicates that the structure exhibit highly heterogeneous behavior that could be less efficient. For the 3x3 patterns, results indicate that 500% reinforcement can be obtained with less than 50%, 75%, and 250% weight increments for diamond, auxetic, and triangular structures respectively. This clearly implies that the selective reinforcement method is more effective for the diamond and auxetic structures as compared to the triangular structures.

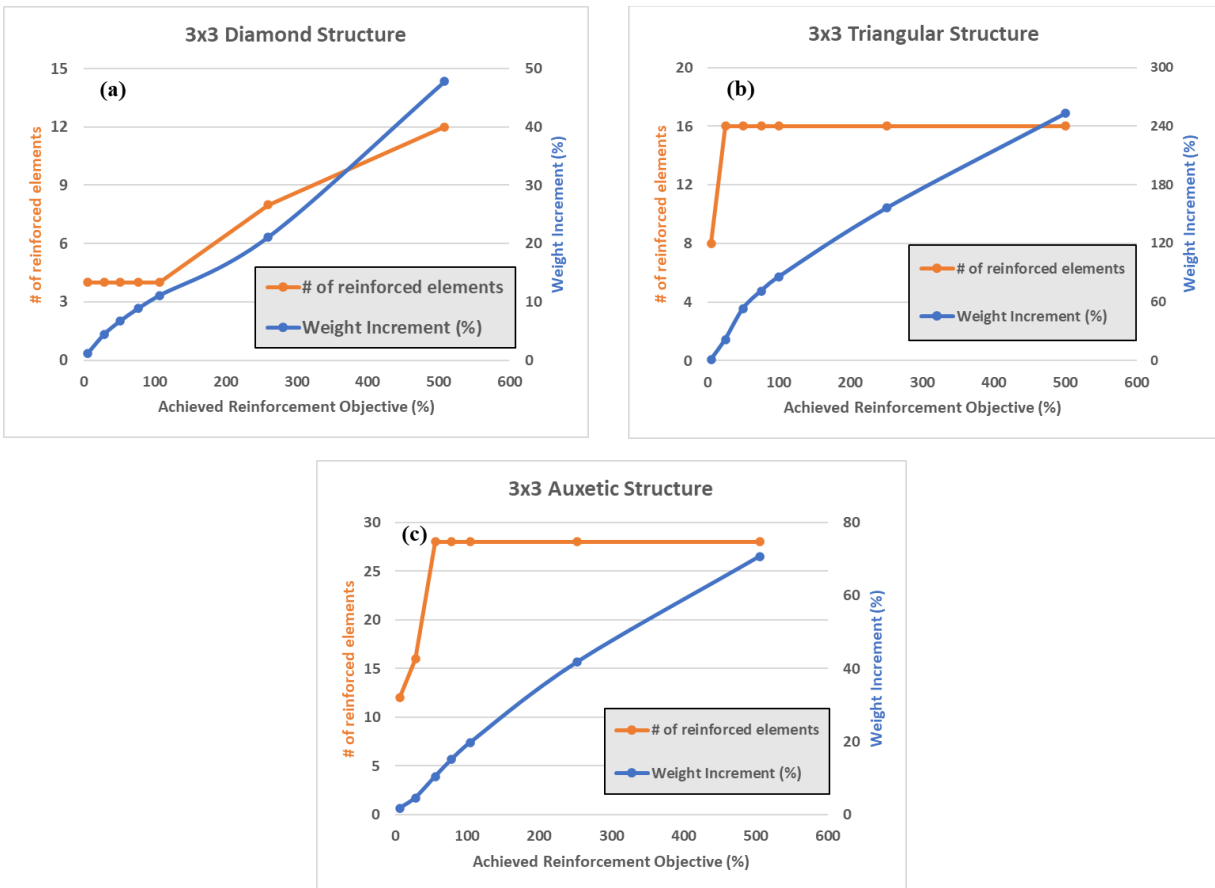


**Fig. 15** Weight increment and number of reinforced elements at different reinforcement levels in different structures

### 3.4. Effect of pattern size on reinforcement

The effect of pattern size with different cellular topology designs is presented in Fig. 16 at 100% reinforcement level. With increasing pattern size, the maximum strength of diamond and triangular structures showed small decreasing trend, whereas the auxetic structure exhibited a very small increasing trend. Also, the 10x10 diamond structure appear to have significantly lower strength compared to rest of the diamond structure with smaller pattern sizes. During investigation, the first failure step of the original 10x10 diamond structure was found to occur at significantly lower stress level, which resulted in lower strength after the 100% reinforcement compared to the other pattern sizes. Although not verified within this study, it was speculated that at very large pattern size the stress concentration at the center of the structure (Fig.4) becomes dominated by the other more critical elements at different locations.

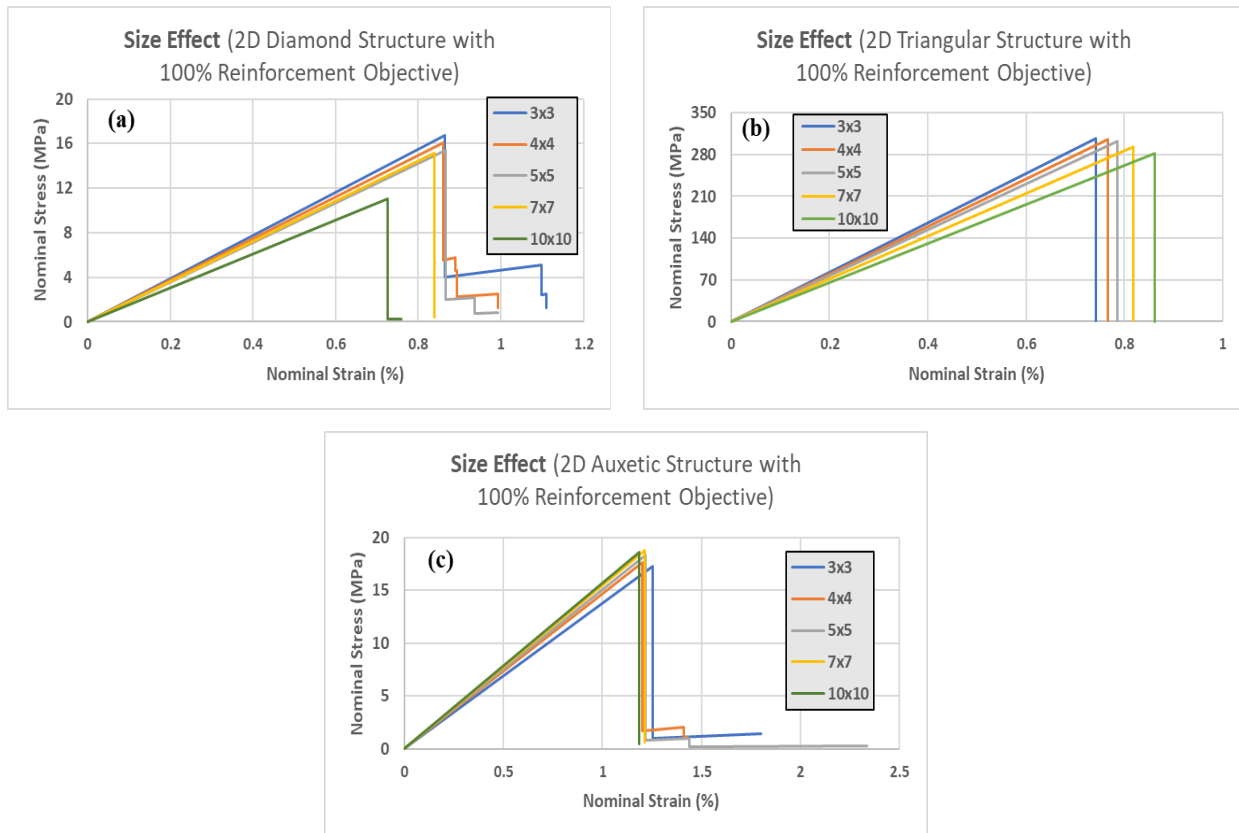


**Fig. 16** Pattern size effect with stress-strain curves at 100% reinforcement level

For both diamond and triangular structures, the larger pattern size corresponds to smaller overall weight increase percentage at constant reinforcement level, whereas the auxetic structure exhibits the opposite trend (Fig. 17). In addition, for all three designs, with larger pattern size generally more elements become reinforced. While it is intuitive that with larger pattern size more elements could potentially become critical and thus need reinforcement, the three structures exhibit different characteristics. The diamond structure exhibits the same number of reinforced elements until the pattern size becomes larger than 5, indicating that there exists a threshold for the central critical elements (see Fig. 4) to become significantly less dominant. With the triangular structure, the number of reinforced elements increases almost proportionally with the increase of the pattern size, suggesting a relatively consistent structural behavior. The reduced weight increment

percentage also indicates that individual elements require less reinforcement, which could likely be explained by the existing notion with the size effects of cellular structures that larger pattern size corresponds to smaller stress concentration effects. In comparison, with the auxetic structure, there exist a very significant increase of the number of reinforced elements as the pattern size increases, with the weight increase following almost the same trend. This suggests that the stress distribution within the auxetic structures is much less heterogeneous, which also agrees with the existing notion with this type of structure.

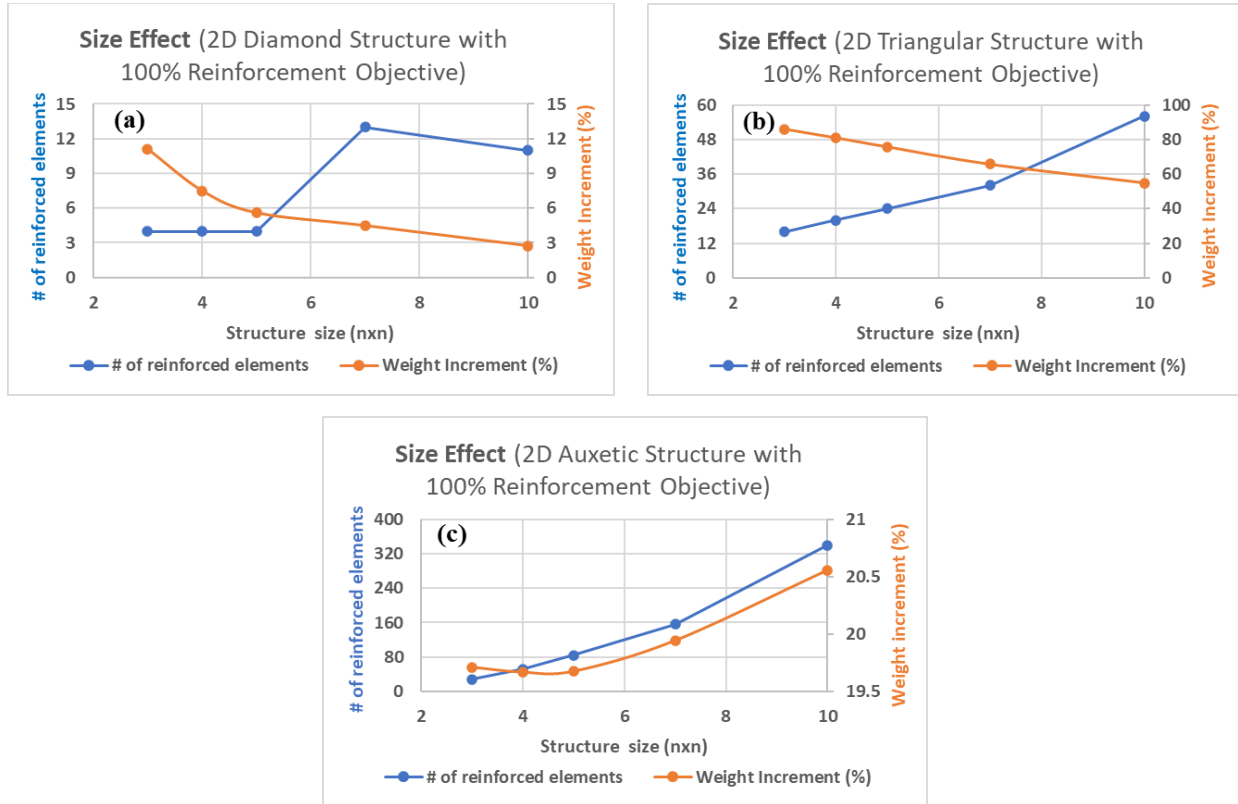


Fig. 17 Pattern size effect on reinforcement effectiveness at 100% reinforcement level

#### 4. Conclusion

In this study, the strength enhancement approaches for 2D periodic cellular structures were explored through selective reinforcement of individual critical elements thickness based on analytical modeling. For the ease of analysis with the reinforcement methods, perfectly elastic material properties were used for the study. It was found that the reinforcement strategy based on only the most critical elements is generally more efficient than the strategy that reinforces throughout the entire fracture path. The results clearly suggest that in addition to reinforcing the strength of the structures, the reinforcement strategy also introduces various change of the structural characteristics, such as fracture pattern and overall weight. The reinforcement process also revealed potential change of criticality mechanisms for certain designs (diamond in this study), which can be useful for future failure characteristic design with cellular structures. Finally, additional studies are needed to improve the accuracy of the model for real-world AM materials.

## Declaration of Competing Interest

The authors declare no conflict of interest.

## Acknowledgments

The authors like to thank Additive Manufacturing Institute of Science & Technology (AMIST) center at the University of Louisville for providing resources for conducting experimental works for this project.

## References

1. Wang, P., et al., *Bio-inspired vertex modified lattice with enhanced mechanical properties*. International Journal of Mechanical Sciences, 2023. **244**: p. 108081.
2. Guo, M.-F., H. Yang, and L. Ma, *3D lightweight double arrow-head plate-lattice auxetic structures with enhanced stiffness and energy absorption performance*. Composite Structures, 2022. **290**: p. 115484.
3. Ghuku, S. and T. Mukhopadhyay, *On enhancing mode-dependent failure strength under large deformation: The concept of anti-curvature in honeycomb lattices*. Composite Structures, 2023. **305**: p. 116318.
4. Xiao, L. and W. Song, *Additively-manufactured functionally graded Ti-6Al-4V lattice structures with high strength under static and dynamic loading: Experiments*. International Journal of Impact Engineering, 2018. **111**: p. 255-272.
5. Shu, X., et al., *Toughness enhancement of honeycomb lattice structures through heterogeneous design*. Materials & Design, 2022. **217**: p. 110604.
6. Song, K., et al., *Crystal-twinning inspired lattice metamaterial for high stiffness, strength, and toughness*. Materials & Design, 2022. **221**: p. 110916.
7. Günaydin, K., C. Rea, and Z. Kazancı, *Energy absorption enhancement of additively manufactured hexagonal and re-entrant (auxetic) lattice structures by using multi-material reinforcements*. Additive Manufacturing, 2022. **59**: p. 103076.
8. Zhang, J., et al., *Enhancing specific energy absorption of additively manufactured titanium lattice structures through simultaneous manipulation of architecture and constituent material*. Additive Manufacturing, 2022. **55**: p. 102887.
9. Yang, X., et al., *Ultra-high specific strength Ti6Al4V alloy lattice material manufactured via selective laser melting*. Materials Science and Engineering: A, 2022. **840**: p. 142956.
10. Li, X., et al., *Heterogeneously tempered martensitic high strength steel by selective laser melting and its micro-lattice: Processing, microstructure, superior performance and mechanisms*. Materials & Design, 2019. **178**: p. 107881.
11. Xue, Y., W. Wang, and F. Han, *Enhanced compressive mechanical properties of aluminum based auxetic lattice structures filled with polymers*. Composites Part B: Engineering, 2019. **171**: p. 183-191.
12. Lipperman, F., M.B. Fuchs, and M. Ryvkin, *Stress localization and strength optimization of frame material with periodic microstructure*. Computer methods in applied mechanics and engineering, 2008. **197**(45-48): p. 4016-4026.
13. Zhang, C., et al., *A novel lattice structure topology optimization method with extreme anisotropic lattice properties*. Journal of Computational Design and Engineering, 2021. **8**(5): p. 1367-1390.
14. Isanaka, B.R., et al., *On exploiting machine learning for failure pattern driven strength enhancement of honeycomb lattices*. Acta Materialia, 2022. **239**: p. 118226.
15. Wu, Y. and L. Yang, *The effect of unit cell size and topology on tensile failure behavior of 2D lattice structures*. International Journal of Mechanical Sciences, 2020. **170**: p. 105342.
16. Wu, Y. and L. Yang, *Modeling and analysis of material anisotropy-topology effects of 3D cellular structures fabricated by powder bed fusion additive manufacturing*. International Journal of Mechanical Sciences, 2021. **197**: p. 106325.